Jasiūnas, Justinas; Lund, Peter D.; Mikkola, Jani; Koskela, Liinu

Linking socio-economic aspects to power system disruption models

Published in:
Energy

DOI:
10.1016/j.energy.2021.119928

Published: 01/05/2021

Document Version
Publisher's PDF, also known as Version of record

Energy 222 (2021) 119928

Contents lists available at ScienceDirect

Energy

journal homepage: www.elsevier.com/locate/energy

Linking socio-economic aspects to power system disruption models

Justinas Jasiūnas*, Peter D. Lund, Jani Mikkola, Liinu Koskela

Aalto University School of Science, New Energy Technologies Group, P.O.Box 15100, FI-00076, Aalto, Espoo, Finland

ARTICLE INFO

Article history:
Received 19 August 2020
Received in revised form
12 January 2021
Accepted 19 January 2021
Available online 22 January 2021

Keywords:
Resilience
Energy security
Extreme weather
Power system
Outage costs
Socio-economic impacts

ABSTRACT

Increasing reliance on uninterrupted electricity supply against emerging threats such as climate change and cyberattacks calls for higher resilience of societies against power disruptions. A better understanding of social and economic impacts during these disruptions would be important for planning of resilience improvements. However, traditional energy system models rarely include these aspects. This paper presents an integrated framework containing a geospatial power system operation model, capable of emulating system component failures and restoration according to environmental conditions, with a link to spatial social and economic values such as population, economic activity, critical services and facilities. The framework was applied for analyzing the effects of uncontrolled and controlled power outages for two windy winter weeks in Finland. This case illustrated how controlled optimization could reduce the societal costs of such outage by shifting power shortage to regions where such costs are lower and in part by shifting the costs to other factors.

1. Introduction

Modern societies rely on a continuous supply of energy and electricity in particular. Disruptions in electricity supply pose a risk of stopping important activities in the society, which could disable many critical services ranging from heating to healthcare or access to drinking water. Exposure to such risks continues to increase due to ongoing electrification and digitalization [1] that are driven in part by the clean energy transition [2]. There are also new types of threats emerging, e.g. climate change and cyberattacks. With the number of weather-related threats being historically among the dominant causes of power outages [3], the energy sector is among the most vulnerable sectors to climate change [4]. Changes in both extreme and typical weather patterns expose long-lived and capital-intensive infrastructures throughout the supply chain [5] to conditions that they were not necessarily designed for. This is especially relevant for systems dominated by weather dependent renewables as the interannual variation of their output is often larger than that of consumption [6]. At the same time increasing digitalization increases the attack surface [1] for cyberattacks from increasingly sophisticated malicious software [7] and increasingly well-funded adversaries [8]. Potential impacts of such attacks range from local data loss to widespread blackouts and physical damage [9]. Both increasing importance of power systems and threats to it call for higher power system resilience, i.e. increasing ability to prevent, minimize negative impacts of, recover and learn from power system disruption events [10].

Addressing the multitude of potential threats to power systems [11] requires complex considerations when making infrastructure investment decisions, developing rules for system operation, and preparing contingency strategies for extreme situations when quick decisions and actions are needed. To aid these considerations, insights about system behavior under disruptions obtained from energy system models could be of high importance. Numerous energy system models exist that deal with techno-economic optimization of capacity installation and its dispatch under different limitations and boundary conditions [12]. While the majority of them primarily focus on operation under normal conditions, some models do account for disruptions providing associated loss of load among output parameters [12]. Some technically detailed power system models can represent system component failures and restoration linked to environmental conditions [13]. However, these models rarely include links to social and economic systems [14] that could be important for decision making, especially when power systems face extreme disruptions. For example, in case of insufficient power supply, a decision may be needed on which parts of the grid would be left without power. While such decisions involve major societal and economic consequences, conflicting values may not lead to straightforward optimization, but to open policy questions [15].

* Corresponding author.
E-mail address: justinas.jasiunas@aalto.fi (J. Jasiūnas).

https://doi.org/10.1016/j.energy.2021.119928

Nomenclature

VoLL	Value of Lost Load
TG	Transmission Grid
DG	Distribution Grid
LG	Local Grid
CHP	Combined Heat and Power
DH	District Heating
GVA	Gross Value Added

The impact of power system interruptions is mostly studied using technical and economic indicators. Technical indicators focus on duration, frequency, number of customers affected, and total unserved energy of disruptions. Commonly used technical indicators are defined in the IEEE standard 1366–2012 [16]. Objective and relatively easy-to-obtain technical indicators do not fully capture demand side aspects that greatly affect the economic costs of disruption, which are often referred to as the value of lost load (abbr. VoLL). VoLL represents a large variety of costs for the same unit of unserved energy depending on the consumer type, timing and duration of the disruption, existence of prior warning and mitigation measures, and other aspects [17]. In addition to a set of aspects considered, the VoLL can differ based on the evaluation method used that include willingness to pay and willingness to accept surveys, detailed analysis of historical disruption cases or indirect analysis using already widely available public data (e.g. gross domestic product) [18]. VoLL is considered to be an indicator of the optimal level of investment in supply security measures [19]. It is also used as one of the cost components in various optimization studies for investment in transmission [20] and generation [21] capacity as well as generation capacity commitment and dispatch [22]. However, the literature that would use VoLL to address social dilemmas or the links of technical energy system models to social values is limited.

Two previous studies present a good example on how VoLL could be used to inform decisions concerning power systems under disruptions while highlighting social dilemmas of different strategies. De Nooij et al. investigated ways to reduce social costs of a 4-h long 1 GW power shortage in the Netherlands by cutting off the power supply of the municipalities with the lowest VoLL in comparison to random rationing [23]. Wolf et al. investigated a 1-h long 10 GW shortage in German districts by rationing supply randomly, minimizing the total cost, minimizing the cost of most affected regions, and minimizing the number of people affected [24]. Neither of the two studies mentions grid constraints of distributing supply or grid damage that would accompany many disruptions causing a shortage on the supply side. Also, not all social values can be represented well in monetary terms [25] (e.g. hospitalized people are not working and thus likely to have a low VoLL [26]). Mentioned aspects show that many important aspects concerning the link between electric power and social or socio-economic systems remain open.

This paper presents a modeling framework that links the technical power system operation model with economic and social values that requires a power supply and can be represented spatially. The objective is an integrated tool for researching: (1) social and economic costs of extreme disruptions to power systems, (2) regional and different value tradeoffs for these costs, (3) effectiveness of proactive and reactive power system resilience improvement measures in reducing these costs. Section 2 describes the framework, Section 3 describes the power system model, Section 4 describes an illustrative case that applies the framework for the Finnish power system, Section 5 concludes the work.

2. Linking framework

Several models link power system operation to various energy security aspects [27,28], but attempts to link power disruptions to socio-economic systems are rare. To enhance the capability to analyze complex and multi-disciplinary socio-economic phenomena that arise in power system disruptions, a framework shown in Fig. 1 is proposed.

The energy security environment layer includes a multitude of threats that differ significantly in the way they affect the power system [11]. Thus, the types of threats considered shape the aspects needed in a representative model. Among all threat types, the majority of disruptions recorded originate from extreme weather events [3]. The link between the weather and the power system on operational time scales requires only performance functions dependent on the weather parameters for each system component. The same link on a longer time scale presents additional complexity related to infrastructure capacity buildup and retirement as well as potential changes in the climate. Traditional energy security typically concerned with fuel embargo requires a model that describes the fuel stocks. Effects from cyberattacks on digital sub-systems depend on the details of adversaries [1], malware and antimalware software [7], logical domains and communication networks within the power system [29]. In the case of cyberattacks the consideration of only the physical part of the system may not be adequate as cyberattacks could e.g. block or inject false data into the digital part of the power system interfering with central control or manipulating the behavior of independent producers and "smart" consumers [30]. However, implications of disabled power system components or changed consumption levels due to such disruptions can be modeled without detailed knowledge about the origin of these incidents. Considering the relevance and modeling complexity of different threats, here the focus of this work is on extreme weather events and disruptions that can be emulated by user imposed power system component failures.

The core layer of the framework is a spatial power system model for a defined geographical area covering production, consumption, and connecting power grid components. Power system components are subject to disturbances altering both the momentary supply capabilities and demand patterns until the system is restored. The damaged system would continue to operate based on predefined rules, which represent different strategies for operating disrupted systems. These strategies may include value judgments, especially when the operational system capabilities cannot cover the whole demand. For example, power supply in one region could be restored by compromising other less important regions. Further details of the power system model are presented in Section 3.

The socio-economic system layer consists of a set of layers with spatial social and economic values that are linked to a power supply system. Examples of such values include population and its structure (e.g. share of particularly vulnerable population due to age, medical or financial situation [31]), industrial and other economic activities, critical services (e.g. communication, water and food supply [32]) and facilities (e.g. hospitals), community capacity to support recovery process [33] (e.g. information availability to mobilize and organize volunteers). The inability of a damaged power system to meet the local power demand incurs socio-economic costs, which can be assessed for each area covered by the grid. Socio-economic costs are considered separately for different values of interest rather than converting all of them into monetary units as it is done in VoLL estimates. The purpose of such an approach is to investigate tradeoffs between different values that could be, at least in part, hidden when all relevant values are expressed in monetary

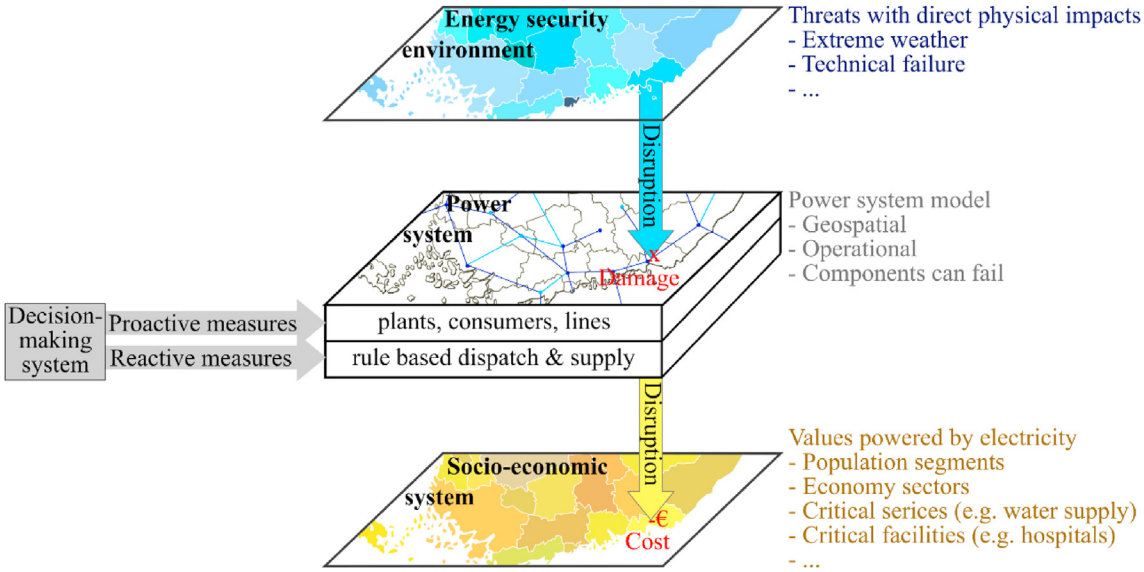

Fig. 1. Framework for linking disruptions to power systems with socio-economic aspects.

units. For example, consideration for power rationing between businesses and residents in VoLL terms would depend on the value set for economic activity and residents' activities outside of work. While it is easier to cut off the power supply for a whole region than for a specific group of consumers in the region [23], VoLLs and their time dependencies between sectors can vary even more than they vary between regions [34]. Even if outage cannot be constrained to specific sector the choice of the region for supply priority may involve similar dilemmas due to the dominant consumer type differences. Keeping relevant socio-economic values separate also can be useful for studying more extreme (in scale and duration) disruptions, where monetary cost is no longer the most relevant indicator. In very long and widespread power outages, where critical services like food supply could become an issue, economic considerations of everyday business are likely to be of lesser importance for operational decisions. However, such long disruptions are outside the scope of the current model mainly due to missing representation of back-up or emergency power generation and fuel stocks in the model. Most critical services have back-up generators with a few days of fuel supply, which could be further resupplied [35]. Disruptions from the socio-economic systems to the power systems (e.g. severe epidemic preventing personnel from operating the power system [3]) are considered as a part of the energy security environment. Potential feedback loops between the socio-economic layers are not considered in the model.

The decision-making system in Fig. 1 represents policy measures that have a major impact on the resilience of the energy system. Proactive policy measures for resilience improvements could include a long-term buildup of infrastructure and operational strategies aiming to prevent disruptions. Strategies prepared in advance, even when they have to be modified in actual situations, can noticeably improve the operational decisions under time pressure during the disruption [36]. Reactive resilience improvement measures primarily comprise operational decisions and infrastructure recovery aiming at mitigation of disruption effects and quick system recovery. Resilience improvement measures acting on the socio-economic system and energy system threats in its environment are outside the scope of the model. In this paper, the model is used with predefined rules, which do not clearly distinguish between decisions made in advance and during the disruption. However, most of the proactive measures are likely to focus on the physical infrastructure, whereas the reactive measures are likely to focus on the operational rules and decisions as changes in long-lived infrastructures outlast the time needed to change the rules. One possible model extension to increase the distinction between proactive and reactive measures would be to interrupt the model run at the point of component failure for further user input.

3. Power system model

The power system model used here is based on maintaining demand-supply balance by dispatching power plants and serving consumers based on respective priority orders defined prior to the model run. The model runs at time scales that can capture the performance dynamics of the system in case of disruptions. It is coded with MATLAB©.

3.1. Power system structure

The power system is modeled as a two-level network shown in Fig. 2. The first level network covers the whole studied region divided into areas with a single node in each. These nodes represent substations in the transmission grid (TG). The second level network consists of local grids (LGs) within each area. Each LG includes plant and consumer nodes connected by LG lines to TG (i.e. area) node. Plant nodes refer to sites of power plants. Consumer nodes represent aggregated distribution grids (DGs) as well as major industrial consumers in the area. For simplicity, both DG and TG lines that fall entirely within a single area are referred to as LG

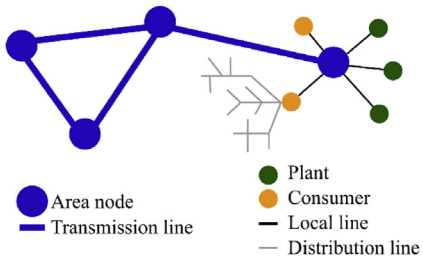

Fig. 2. Illustration of the power grid structure in the model.

lines in the rest of the text. Cross-border connections are represented with dummy area nodes containing a dummy plant for imports and a dummy consumer for exports. TG can include several loops, but LG is assumed to be non-looped (DGs typically have a tree-like topology [37,38]) to limit the complexity and computational requirements of the model.

Each plant and consumer node include specific information on their characteristics about their location, sub-type, power characteristics, and distribution impacts as listed in Table 1. The location of the node within the grid is specified by the corresponding area (transmission) node and upstream and downstream lines of the corresponding LG. Plant nodes are categorized according to the energy source or fuel used, while the consumer sub-types represent different sectors such as households, services, and industries. Each consumer node contains consumers from one type of sector only, i.e. DG serving multiple types of consumers is aggregated into separate consumer nodes with each node representing a sector within given DG. Power characteristics distinguish between nominal and actual values after balancing the power system. Power production is also subject to minimum and maximum operational plant output and availability. Availability refers here to maximum production capacity at different plant damage levels and grid constraints. Disruption impacts on the power plants are described through fragility functions and fixing times [39]. A component and threat specific fragility function links failure probability to the intensity of the disruption describing parameter. For example, extreme weather disruption could be described by weather parameters such as temperature, amount of rainfall, or wind speed in the area, where the power system component is located (see Fig. 3). Fixing time defines the time lag until the plant returns to operation after a breakdown or black-out. Disruption impacts on consumers are represented indirectly through social and socio-economic parameters sensitive to power disruptions.

Table 2 lists model variables for the rest of the system components – LG and TG lines, and TG node. Both LG and TG lines are described by their location with nodes at their ends, power carrying capacity, and actual power flow. The model also includes representation of LG line failure in the same way as for power plant failures, i.e. using a fragility function, fixing time, and reduced availability of power carrying capacity. The current model setup, however, does not include endogenous representation of the TG line failures due to the need to reconfigure looped TG for the calculation algorithm used. To simulate TG line failures, the user has to manually modify the system components before the model run. Another unique feature about TG lines is the distinction made for computational reasons between straight or loop-forming lines (details in the next subsection). Each TG node is specified by its location as well as the total electricity production and consumption connected to that node.

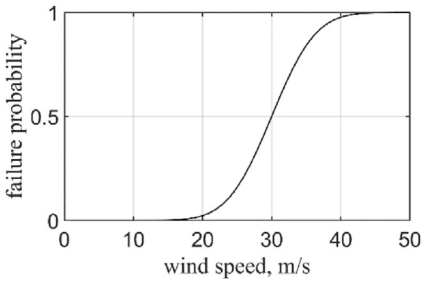

Fig. 3. Example of a fragility function (failure probability as a function of wind speed).

3.2. Calculation principles

The model computes the state of the power system for each time step (typically 1 h) using an algorithm with four main parts as shown in the central part of Fig. 4 based on [40–42].

First, the model calculates the availability of each plant and line in the LG. The availability of these components is equal to their capacity in a normal state and zero in a failed state. Failure is determined by comparing the failure probability with a randomly generated number from a uniform distribution. The failure probability of component is defined by its fragility function and environmental conditions. Once the component fails, it is assigned a timer with a predefined value that decreases every subsequent time step. After the timer reaches zero, the component is fixed and its capacity is restored.

The second part of the model sets the production, consumption, and power flow levels without considering the grid constraints. The power plants are dispatched and consumers supplied based on their respective priority orders until the supply-demand balance is reached. The power plant priority represents the rules of a free power market, based on the marginal costs of power production and additional rules such as the preference for low emission sources. The consumer priority order is based on socio-economic values defined by the user. Assuming that the LG is not looped, i.e. it has a radial or tree-like topology [43], flow in LG lines is defined by cumulative downstream production and consumption [42] as follows:

$$F_l = \sum_{n \in ds(l)} (Q_n - P_n) \tag{1}$$

where F_l is the power flow in LG line l, Q_n and P_n are the power consumption and production in node n. The notation $ds(l)$ means the nodes that are downstream (i.e. further from the transformer station) of line l. Positive numbers mean downstream flow, negative ones – upstream.

Table 1
Model variables for power production and consumption nodes.

	Plant node		Consumer node	
Location	Area node		Area node	
	Upstream line		Upstream line	
	Downstream line		Downstream line	
Sub-type	Power plant type	[energy source]	Consumer type	[sector]
Power characteristics	Maximum production capacity	[MW]	Demand	[MW]
	Minimum output	[MW]		
	Availability	[MW]		
	Actual production	[MW]	Actual consumption	[MW]
Disruption impacts	Fragility function		Population	[people]
	Fixing time	[h]	Gross value added	[€]
			Jobs	[people]
			etc.	

Table 2
Model variables for the remaining power grid components.

Local grid line		Transmission grid line		Transmission grid node	
Area node				Area node	
End nodes		End nodes		Upstream line	
Capacity	[MW]	Capacity	[MW]	Downstream line	
Actual flow	[MW]	Actual flow	[MW]	Geographical location	
Fragility function		Line type		Production in the local grid	[MW]
Fixing time	[h]			Consumption in the local grid	[MW]
Availability	[MW]				

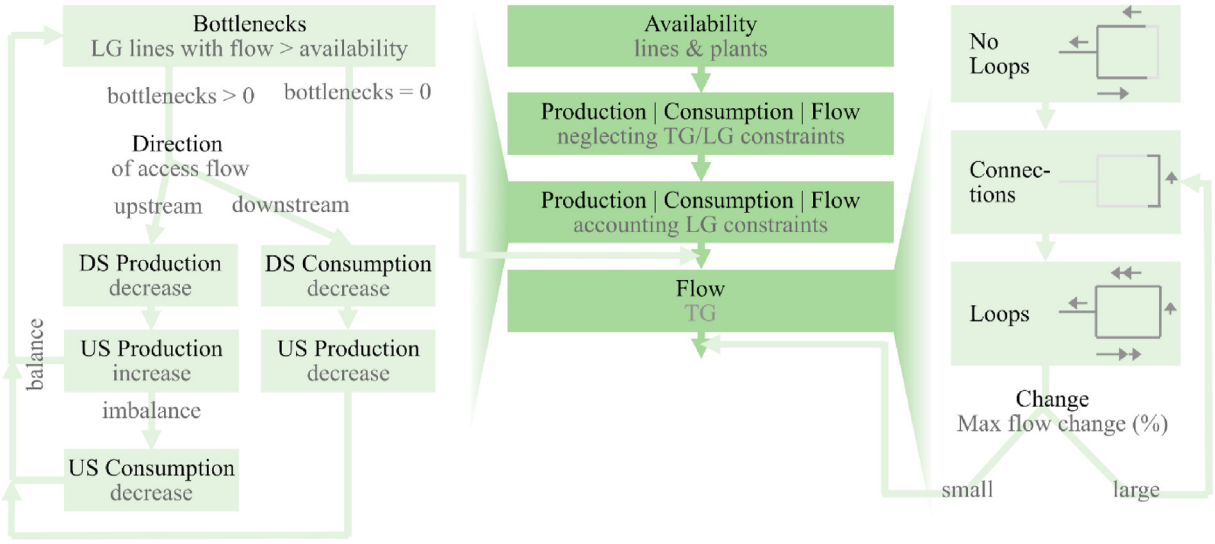

Fig. 4. Principle scheme of the power system model algorithm. Notations used: DS – downstream, US – upstream.

The third part of the model adjusts production, consumption levels taking into account the LG constraints. The principal scheme of this step is further detailed on the left side of Fig. 4. The LG lines with flows larger than their availability (power carrying capacity that can be reduced in case of failure) represent bottlenecks. Each bottleneck is removed individually by adjusting production and consumption levels downstream and upstream of the line based on excess flow direction. First production and consumption levels are adjusted downstream, and then, to retain a supply-demand balance of the system, upstream. Each removal of the bottleneck can create new bottlenecks. Therefore, after removing the initial set of bottlenecks the third part of the model is repeated until no more bottlenecks are found. To avoid infinite loops, the model does not allow increasing values of power plant production that were already reduced during that time step.

The fourth part of the model computes the flows in TG that differ from the LG by the presence of loops. The principal scheme of this step is detailed on the right side of Fig. 4. Initially, the model omits certain lines in TG eliminating loops that allow computing flows in each line by summing downstream production and consumption using Eq. (1). After that, the flow in omitted loop-forming lines is computed based on the voltage differences between the neighboring nodes [40,42]:

$$F_{lf} = -\frac{\sum_{l=1}^{L} F_l R_l - \sum_{l'=1}^{L'} F'_{l'} R'_{l'}}{\sum_{l=1}^{L} R_l + \sum_{l'=1}^{L'} R'_{l'} + R_{lf}} \quad (2)$$

where R is the resistance, F the power flow, subscript l refers to the lines in the first branch from the substation (L in total), and l' and L' refer respectively to the second branch, lf = loop forming line. For a detailed derivation of the equation see Supplementary Information. Addition of flow F_{lf} to the rest of the lines in the loop gives a complete description of the flows in the loop. However, when several loops are present in the system, loops can affect each other requiring an iterative calculation. In such a case, the model calculates the flows in the loops one by one and after one round of calculation checks the flow changes. If the maximum change of the flow in relative terms is higher than the predefined precision value, the fourth part of the model is repeated taking new flow values for the loop non-forming lines. Otherwise, the model calculations for the current time step are completed.

At the end of each time step, the history of time dependent variables is saved for further analysis and for socio-economic cost evaluation which is preformed after the power system model run for the whole studied period.

3.3. Model limitations

The central limitation of the model is that it leaves the link between the security environment and the social system layers largely exogenous capturing these relations only through rather simple functions. For the purposes of studying different power systems configurations and operational strategies to reduce socio-economic costs of disruptions, only the internal dynamics of the power system have to be modeled endogenously. However, for an accurate representation of the socio-economic impacts from a disruption to the power system, links between the layers are as important as the internal representation of the power system. Linking functions do allow to capture the major relationships but determining these functions accurately can be very challenging in a

macro level model. A notable simplification is the aggregation of regional DGs or their segments into single point consumer connected via LG line to TG.

Other notable limitations of the model concern three aspects: time scale, grid topology, and intermediate states of the system components. First, the focus of the hourly time scale used here does not allow the model to capture near-real-time ($\Delta t \ll 1$ h) power dynamics as well as very long-term ($\Delta t \gg 1$ year) structural changes in the electricity system and its environment. Second, the grid topology limitations concern the representation of disconnected parts and the number of loops in the grid as well as detail in the LGs. Multiple disconnected parts of the system, i.e. power system "islands", that could form due to the main power line failure [44], are outside the model capability. The model also limits the number of loops in the grid due to quickly increasing computational requirements and the need for more sophisticated mathematical approaches to mediate such an increase [45]. The loop constraint applies to both the TG and LG, but at this stage, the LGs are represented without any loops. A very detailed description of the LG could lead to overwhelming complexity and inflate the main idea of the present model. Third, the intermediate state limitations refer to the exclusion of transient conditions and partial failures. The absence of transient conditions makes the system more flexible than it would be in reality. Partial failures could be relevant in cases where the power plant consists of several independent units and the grid line consists of several parallel lines while the disruption impacts only a single unit or line. The possibility of partial failures could also provide more accurate representation of aggregated components. For example, partial failure of a LG line that serves "aggregated DG consumer" could represent a minor line failure in the DG even if no line in that grid have a partial failure state. However, modeling transient conditions and partial failures requires very detailed information on the infrastructure, which is outside the scope of the present study. The overall impact of mentioned model limitations is difficult to assess. Nonetheless, this impact to accuracy is expected to be sufficiently small to allow a representative study at a macro scale, provided that functions describing links are reasonably representative as well.

4. Illustrative case study of the Finnish power system subject to a disruption

This chapter describes the application of the model for a case study of the Finnish power system during a 'stressed' situation of two windy winter weeks with no possibility of imports and reduced availability of present nuclear power capacity. The aim is to illustrate the application of the framework and model capabilities.

4.1. Description of the disruption

The disruption in this scenario is represented by a storm hitting an already stressed power system. Wind is the biggest cause for most power system disruptions in Finland (e.g. 28% disruptions in 2017 [46]) as in many other countries [3]). The extreme wind primarily damages low and medium voltage power lines that are unlikely to lead to a nation-wide supply shortage in the Finnish power system. However, if the storm hits a stressed power system lacking major supply sources, namely power imports from neighboring countries and present nuclear power capacity in Finland, the resulting damages could be significantly larger.

The hazard of a storm is represented by the wind gust speed for each modeled area equal to the measured gust speed in one randomly selected metrological station among the stations in the corresponding area. Such extrapolation neglects local variations. However, a more accurate representation would need to account for the sub-area distribution of both the wind and power system components, which is outside the scope of the model and present study. The wind gust profiles used for 2-week study period are shown in Fig. 5. The profiles contain several peaks with the longest and the highest peak occurring in the middle of the second week. As it could be expected, the wind speeds are the strongest in the coastal regions. However, the northern part of Finland (Lapland) and, to a lesser extent, the corridor from south to northeast of the country also experience strong winds during the same period.

While strong winds are unlikely to damage cross-border TG lines, extreme weather conditions that cause significant damage in Finland can affect neighboring countries limiting their excess capacity for exports to Finland. Regardless of the cause, the loss of imports would significantly reduce the extra supply capacity available for the system. If this would coincide with two out of four existing Finnish nuclear power plants being offline, the remaining power supply capacity would come close to, and at some periods, below the demand. The nuclear power plants operate with a high capacity factor with most scheduled maintenance taking place during low consumption in the summer. The unavailability of two nuclear plants in January assumed for this scenario would be unlikely without some external cause.

The power system operator can control the location of outage in case of a system-wide supply shortage by directing power flows under grid constraints. These grid constraints can include damaged lines, most notably on the consumer side, i.e. LG lines between TG and consumer. Thus, from the power flow control perspective, disruptions that damage consumer side lines can be seen as uncontrolled disruptions and disruptions that do not – as controlled disruptions. In the studied case the cause for uncontrolled disruptions is line failures on the consumer side due to the storm, the cause for controlled disruptions is a system-wide supply shortage due to limitations on nuclear and import capacity as well as power line failures on the supply side (LG lines connecting power plants to TG). There is part of the lost load that could be attributed to both types of disruptions as LG failures on the demand side reduce available demand and in turn reducing the effective system-wide shortage. This overlapping share of the lost load is considered for further analysis to be caused by line failures as it cannot be reallocated by the power system operators to different consumers.

4.2. Finnish electricity system

The Finnish electricity system contains 17.5 GW of power production capacity [48], 22 500 km of high-voltage, 140 000 km of medium-voltage, and 240 000 km of low-voltage lines [49]. Fig. 6 shows the power supply composition. The total power supply production is distributed around the country: 25% comes from nuclear at Loviisa and Olkiluoto sites (east and south coasts respectively); 15% comes from hydropower, mostly in the northern part of the country; 25% comes from combined heat and power (CHP) plants for district heating (DH) that are concentrated in larger cities (predominantly in western and southern parts of Finland) and industry that is concentrated in large industrial sites (predominantly in central and eastern parts of Finland) [50]. Fig. 7 shows the TG structure and its representation in the model. Finnish TG contains 116 substations [51] while its model representation contains 29 area nodes and 5 transnational trading nodes (connecting Finland with Sweden, Estonia, and Russia). 8 of the nodes (colored in light blue) have consumption only while the rest (colored in dark blue) have both consumption and production. 10 areas correspond to official regions in Finland and 19 areas represent parts of the other 8 official regions. 8 regions are divided in a way that improves the representation of the TG structure and distinguishes largest producers (namely Olkiluoto and Loviisa

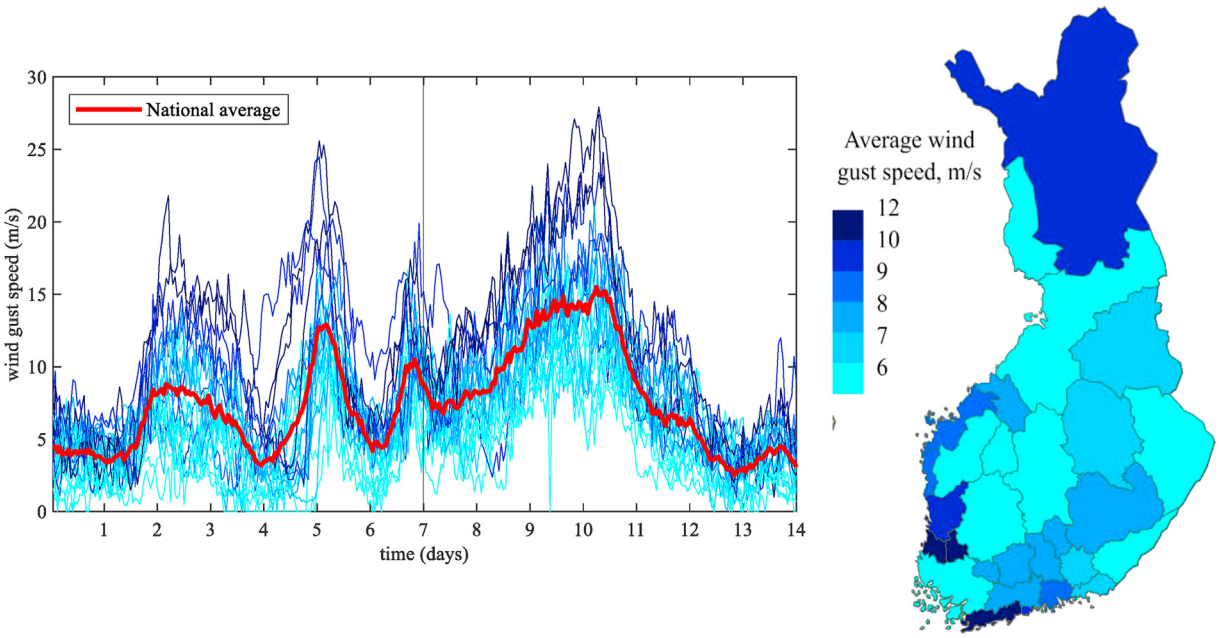

Fig. 5. Wind gust speeds for the first two weeks of 2017: hourly profiles (left side) and regional distribution of their averages (right side). Data source: Finnish Meteorological Institute [47].

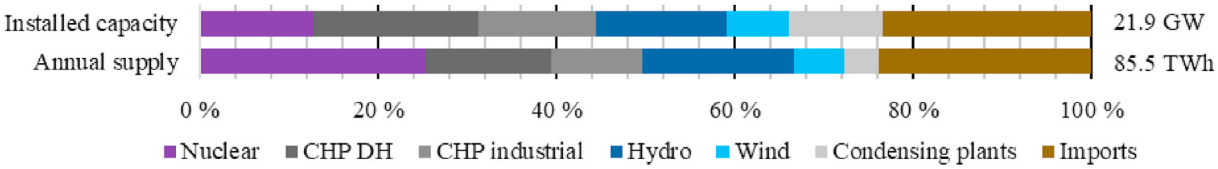

Fig. 6. Installed capacity and an annual supply of electricity in the Finnish power system in 2017 [53]. Condensing plants include peak gas turbines, engine power plants, and condensing shares of combined production. Imports for installed capacity denote the interconnection capacity with neighboring countries. Imports of annual supply are equal to net imports.

nuclear sites) and consumers (most notably Helsinki, capital city) in the system. Åland Islands (west of mainland) were left out from the model because their power system is more strongly linked to Sweden than mainland Finland. The LG follows a radial structure shown in Fig. 8. Fig. 8 also shows the priority order of power plants and consumers used in the model. The power plant priority order is based on the existing merit order on the electricity market. The consumer priority is assumed to be higher for areas with a higher population and within area follow the order shown in Fig. 8. Such order is based on the fact that cutting off the power supply for selected regions in full is technically easier and faster than denying supply for certain consumer sectors over the whole country [23].

The power system data is collected from the following sources: power production and grid data from the national transmission system operator Fingrid Ltd. [48], the geographical distribution of production units from the official power plant register of the Energy Authority of Finland [50], municipal and sectoral composition of consumption from the Finnish Energy [52].

4.3. Inter-layer links

The link between the power system and its natural environment containing the wind hazard is described by the fragility functions and the fixing times of LG lines (failure of TG lines and power plants is not considered in this case). The literature on wind fragility of power systems containing fragility functions for power line towers and line segments connecting were found in Refs. [13,37,39,55,56]. As these functions can be site specific and depend on many component level characteristics (such as line strength, line length, tower age, material of the tower, presence of neighboring components, power loading at the time of the study, presence and nature of other hazards) aggregating all components for a national power system study is challenging. For this illustrative study, the line strength was considered as the main parameter for line fragility. The fragility of higher voltage lines is assumed to have the same failure probability distribution profile as lower voltage lines, just shifted to higher wind speed range. The LG line voltage levels were determined using connected power production capacity or peak demand as a proxy. The fragility functions for this study are assumed to have a normal cumulative distribution with a variation of 5 m/s (see Fig. 9). Distributions were selected considering the rarity of: (1) line failures with wind speeds are < 20 m/s [55], (2) high voltage line failures due to wind in general [13], wind in Finland reaching speeds > 30 m/s. Differences in the line damage and surrounding environment that could affect restoration works are accounted for by fixing the time variation [57,58]. No fixing is allowed during the storm when wind gust speeds are >20 m/s. Also, if the failure occurs during the storm, the base fixing time is multiplied by a random number from a uniform distribution with ranges between 2 and 4. Base fixing times are assumed to be 5/10/20 h for low/medium/large voltage power lines.

The link between the power system and the socio-economic

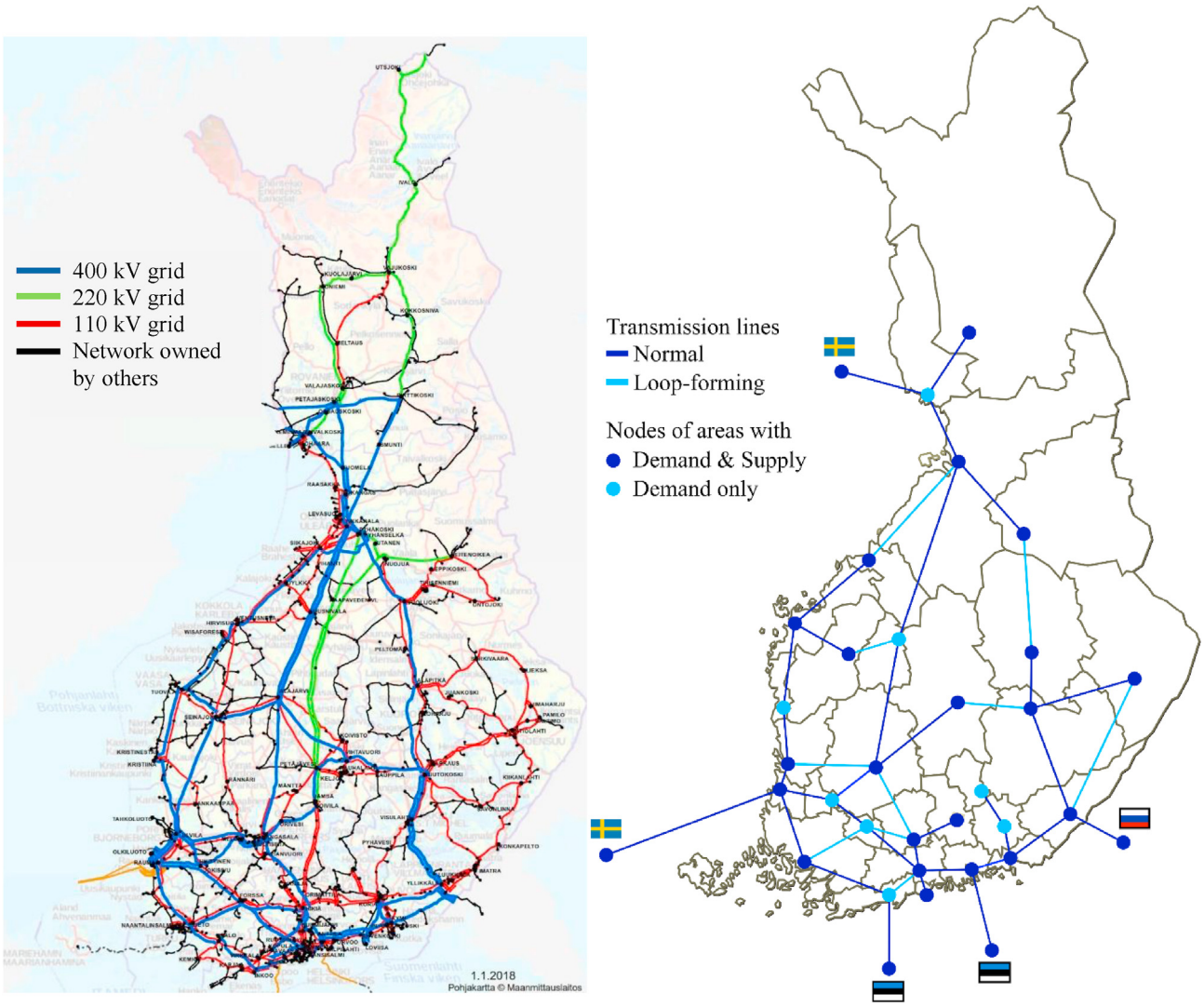

Fig. 7. Finnish power transmission network (left side, the figure is taken with permission from Fingrid Ltd © [54]) and its simplified representation in the model (right side).

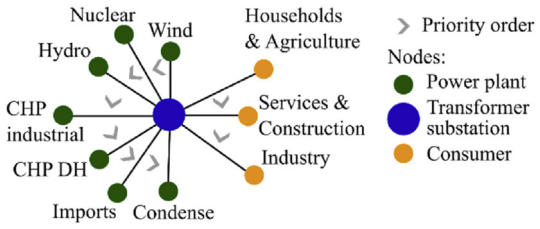

Fig. 8. Simplified local grid structure within an area including all node types and subtypes with their priority orders (indicated with arrows) used in the case study.

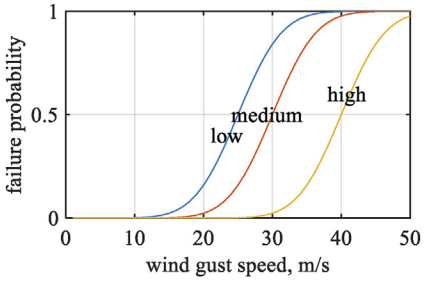

Fig. 9. Fragility functions used for low, medium, and high voltage lines versus wind gust speed.

layers assumes only direct impacts and a uniform distribution of socio-economic values of interest within the areas. In principle, any value with available geospatial data and known dependency on power supply can be studied within the proposed framework. For the purposes of evaluating the cost of major power disruptions, the most relevant values would be related to critical functions and infrastructures for the economy and broader society. There is no broad consensus on what constitute critical infrastructures or functions, though typically such lists are longer for more developed countries [59]. In Finland, the Security Committee identifies the following basic functions of society: water distribution, food supply, financial payments, transportation, telecommunication, heating, and certain public facilities (namely hospitals, emergency response centers, police departments, fire stations, schools and daycare centers) [32]. This illustrative study uses examples of values easily applicable within the proposed framework, namely four socio-economic factors: gross value added (GVA), population, elderly (age over 65 years old and therefore potentially more

vulnerable) population, health and social work jobs as a proxy of healthcare services. The geographical distributions of these values in Finland are shown in Fig. 10.

The share of each disrupted socio-economic value is assumed to be directly proportional to the share of the disrupted power supply for each time step and end-use consumer studied. For the GVA, or other socio-economic values that are accumulated throughout the year, the simplest time period for which that ratio would be computed is a whole year:

$$GVA_{disrupted,c,t} = GVA_{c,a} \cdot \frac{E_{shortage,c,t}}{E_{demand,c,a}} \tag{3}$$

where c = consumer index, t = time step, a = index identifying annual value, E = energy. Summing up Eq. (3) for all C consumers and all timesteps during the study period T gives:

$$GVA_{disrupted} = \sum_{c}^{C}\left(GVA_{c,a} \cdot \frac{\sum_{t}^{T} E_{shortage,c,t}}{E_{demand,c,a}}\right) \tag{4}$$

Disrupted GVA illustrates the disrupted economic activity in monetary terms, e.g. Euros. However, analysis of multiple values with different units is easier in relative terms, i.e. using the ratio of the disrupted value to the maximum value that could be disrupted during the studied period (i.e. during complete blackout):

$$GVA_{\%disrupted} = \frac{\sum_{c}^{C}\left(GVA_{c,a} \cdot \frac{\sum_{t}^{T} E_{shortage,c,t}}{E_{demand,c,a}}\right)}{\sum_{c}^{C}\left(GVA_{c,a} \cdot \frac{\sum_{t}^{T} E_{demand,c,t}}{E_{demand,c,a}}\right)} \tag{5}$$

The rest of the studied socio-economic values are constant throughout the year for which a more intuitive time basis would be the studied time period (the disruption duration could be even a better basis in case of a single clearly defined disruption). For example, similarly defined population *Pop* indicator would show the average number of people without supply over the studied period:

$$Pop_{disrupted,c,t} = Pop_c \cdot \frac{E_{shortage,c,t}}{E_{demand,c,T}} = Pop_c \cdot \frac{E_{shortage,c,t}}{\sum_{t}^{T} E_{demand,c,t}} \tag{6}$$

Eq. (6) sums up to Eq. (7) for each consumer and time step:

$$Pop_{disrupted} = \sum_{c}^{C}\left(Pop_c \cdot \frac{\sum_{t}^{T} E_{shortage,c,t}}{\sum_{t}^{T} E_{demand,c,t}}\right) \tag{7}$$

In case of a complete outage, the maximum disruption affects the whole population (i.e. the energy sums are the same) giving the share of population disrupted as:

$$Pop_{\%disrupted} = \frac{\sum_{c}^{C}\left(Pop_c \cdot \frac{\sum_{t}^{T} E_{shortage,c,t}}{\sum_{t}^{T} E_{demand,c,t}}\right)}{\sum_{c}^{C} Pop_c} \tag{8}$$

Analogously, disrupted elderly population *ElderPop* refers to the average number of people at least 65 years old without power supply during the study period and in relative terms their disrupted share is equal to:

$$ElderPop_{\%disrupted} = \frac{\sum_{c}^{C}\left(ElderPop_c \cdot \frac{\sum_{t}^{T} E_{shortage,c,t}}{\sum_{t}^{T} E_{demand,c,t}}\right)}{\sum_{c}^{C} ElderPop_c} \tag{9}$$

Likewise, disrupted healthcare and social work employees *HealthJobs* refers to the healthcare and social work services disrupted by measuring a proxy of time averaged (over studied period) number of people employed in this sector without power. Accounting for backup power generation in the most critical areas of healthcare sector was beyond the scope of this study. Thus, the disrupted healthcare share is equal to:

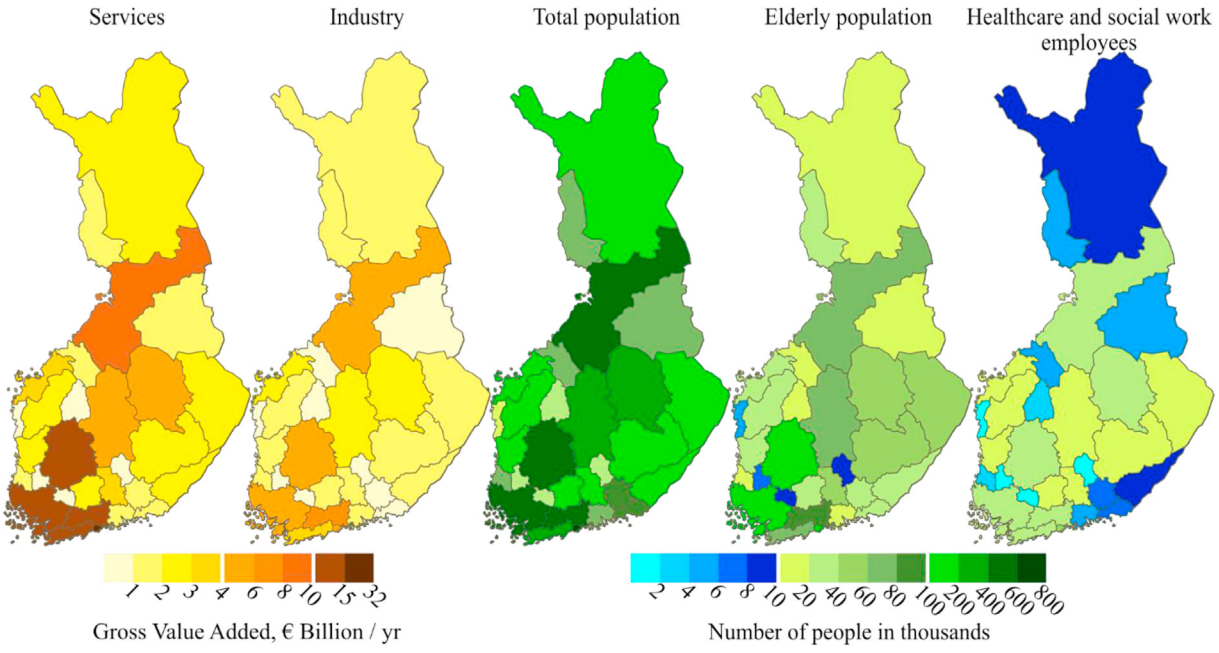

Fig. 10. Geographical distribution of socio-economic values studied in Finland for 2017. Data source: Statistics Finland [60–62].

$$HealthJobs_{\%disrupted} = \frac{\sum_c^C \left(HealthJobs_c \cdot \frac{\sum_t^T E_{shortage,c,t}}{\sum_t^T E_{demand,c,t}} \right)}{\sum_c^C HealthJobs_c}. \quad (10)$$

The energy shortage is the difference between the demand and modeled consumption of energy, while all regional socio-economic data was taken from Statistics Finland [60–62]. The GVA of household consumers is zero and the power loss in this sector does not contribute to the economic impact (no economic value is assigned to the convenience or leisure of residents in the area). As the population of commercial and industrial consumers is zero, the power loss in these sectors does not disrupt population that also includes elderly population (indirect impacts are excluded). Similarly, disruption of healthcare jobs is considered to be caused only by shortages among the service sector consumers.

4.4. Case study period selection

The case study period was selected from years with hourly data available by searching for the largest energy outage that could best illustrate the intended use of the model. Hourly data for gust speeds is provided by the Finnish Meteorological Institute since 2010 [47]. Search for the largest outage that the model could produce included analysis of 10-year wind gust speed data and one-year-long model run. An analysis of the 2010–2019 datasets included simple plotting of national average and a national maximum of wind gust speeds, number of areas and days at which the gust speed is higher than a threshold value. These plots did not reveal obvious peaks in the wind hazard intensity. The model run for year 2017 including the wind hazard but excluding the constraints on nuclear and import capacity resulted in the largest relative energy shortage in the second week of the year. Using this as a basis, the first two weeks were chosen for further analysis with constraints on nuclear and import capacities. Further analysis, shown in the results subsection, replicate the same sequence of power line failures by starting with the same seed for random number generation. The selection of all hourly profiles for a defined period allows to use historical wind power production values without the need to model endogenously connection between wind power production and wind speed.

It is worth noting, that a one-year-long model run without nuclear and import constraints resulted in 0.39% of the annual demand unserved, which is an order of magnitude larger than the actual disruptions in Finland in 2017 [46]. This means that the fragility functions used may be too sensitive for recreating historical wind hazards. However, the decision was made to use oversensitive fragility functions. Thus, the following results present a case that could happen (there are prior storms with a comparable level of disruption in Finnish power system history, e.g. Ref. [63]), but not a historically accurate recreation of events at the start of 2017 in the Finnish power grid.

4.5. Results

Fig. 11 - Fig. 13 shows the evolution of the power system disruption as a function of time. Fig. 11 shows the availability of the power lines with most failures occurring in the second week. The failure rate is significantly higher during the second week despite peak wind gust speeds being only slightly higher that week. This indicates a high system sensitivity to wind speeds once they are sufficiently high to cause component failures as could be expected by wind power being proportional to the cube of wind speed. Failures that do occur in the first week mostly affect the lower capacity lines, primarily on the demand side. Subsequently, almost all of the loss of power production occurs during the second week as shown in Fig. 12 (note that the production capacity loss in the model occurs due to failures in the LG lines connecting plants with the TG rather than failures in the power plants themselves). The power demand during the first week is noticeably larger than during the second one. In the absence of the imports and half of the nuclear capacity available, a higher demand also creates a supply shortage. Fig. 13 shows the impact for the two weeks to be equal in magnitude (share of lost load equal to 2.7% for both weeks, $1.1 + 1.6 = 2.4 + 0.3 = 2.7$), but different in nature (the second week is dominated by line failures while the first week contains line failures and system-wide shortages at comparable level).

Fig. 14 shows the geographical distribution of the modeled disruption impacts. Failures of lower voltage lines resulted in a widespread, but a relatively small amount of lost load. In absolute terms, the lost load is concentrated in a few areas, where the major power line failures occur. In relative terms, however, the lost load is highly concentrated in a few small areas with the lowest priority consumers. While certain areas would be more exposed to line failures due to climate conditions (e.g. windier coastal areas), the spatial distribution of each storm and its impacts is likely to differ. The same may not be the case for the national shortage induced outages if the same prioritization criteria are always used. In addition to this, the time dependency of the damage not considered here could increase the cost over time leading to a rotation of outages between the different regions as a more preferable strategy.

Fig. 14 also shows the nation-wide shares of disrupted socio-economic values which are presented in numerical form in Table 3. The most noticeable aspect of the results is the difference of disrupted values in controlled and uncontrolled disruptions. In controlled disruptions (caused by the national power shortage) all disrupted value shares are lower than the disrupted load share. In uncontrolled disruptions (caused by the power line failures on demand side) the disrupted shares of GVA and healthcare jobs are either close or significantly higher than the share of lost load. This difference is due to the partial shift of the impact to household consumers and regional variation in size of the population, GVA, and energy consumption.

The shift of the lost load to the household consumers is counterintuitive as the system-wide shortage is distributed with household consumers having the highest priority within each area and line failures do not differentiate consumer segments. However, the controlled shortage is distributed first by priority of the area and only then by the consumer types in it. Thus, all but the highest priority areas among the affected ones at any given time are completely cut off. At the same time, most of the shortage caused by the consumer side line failures occurs due to a few large line failures that in this case happen to affect disproportionally industrial and service sector consumers. Among the most affected areas in absolute terms are the Lappeenranta and Inkoo areas (located in the east and south parts of the country) which have high household consumption that in the model is aggregated to large consumer nodes supplied with HV lines that do not fail while the Pori area (on the west coast) is dominated by industrial consumption. This suggests that a longer study period with multiple extreme wind events would likely result in shortage to be more evenly distributed among all sectors in both types of disruptions.

Regional variation in economic output per capita is not large, but economic output per energy unit is. The annual GVA per capita in the studied areas range from 25 138 €/person to 57 723 €/person. The annual GVA per energy unit in the studied areas range from 445 €/MWh to 7643 €/MWh (17-times difference). Most of the GVA per energy unit variation between the areas comes from the industry

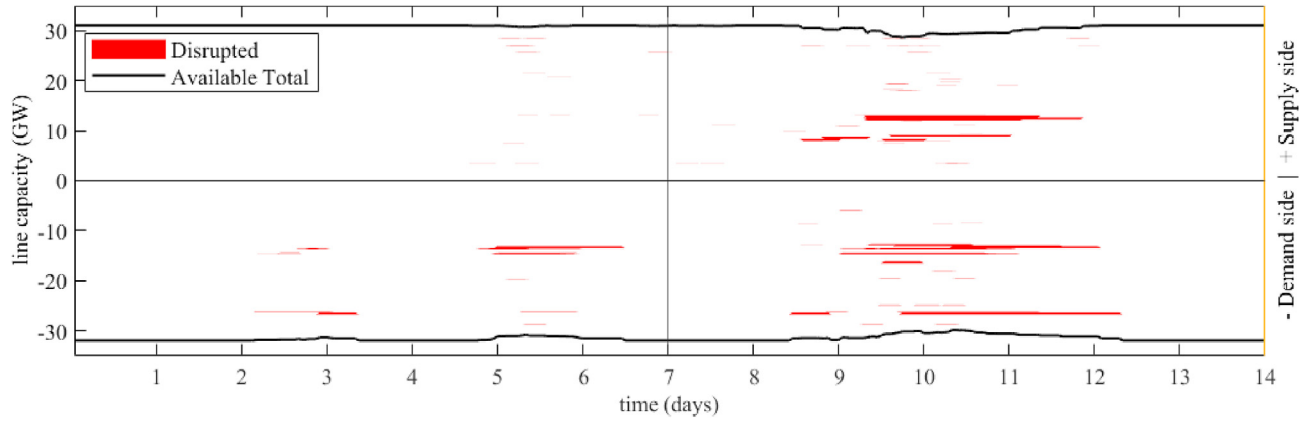

Fig. 11. Availability of local lines (ordered by area).

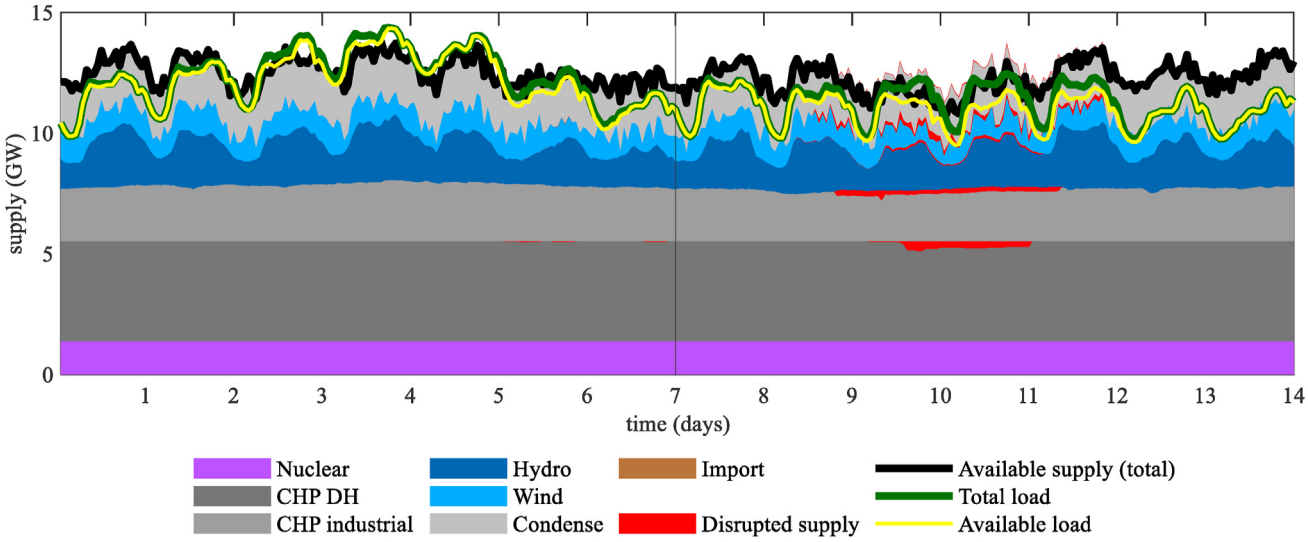

Fig. 12. Availability of the power supply capacity. For clarity purposes, unavailable nuclear power and import capacity (1.3 GW and 5.2 GW respectively) are excluded from the graph.

Fig. 13. Shares of the served and unserved load.

(maximum is 83 times the minimum) while the service sector consumption economic value is relatively uniform throughout the country (maximum is 3 times the minimum). Similarly, healthcare jobs per service sector energy consumption differ among regions by a factor of 3. However, the regional variation of total and elderly population per residential sector consumption differs by a factor of 14 and 7, respectively. Mentioned examples show that economic as well as social impact can be reduced multiple times by shifting the outage location without necessarily shifting the shortage to the other sectors and thus creating different types of costs. This is consistent with the findings that the shortage directed to lower priority areas could significantly reduce the costs compared to a random selection of such areas [23,24].

Two other differences among the results are noticeable. First, the ratios (of disrupted values due to line failures versus disrupted values due to system wide shortages) are higher for all values during the second week as the smaller shortage can be moved to the least valued consumers. Second, the disrupted elderly

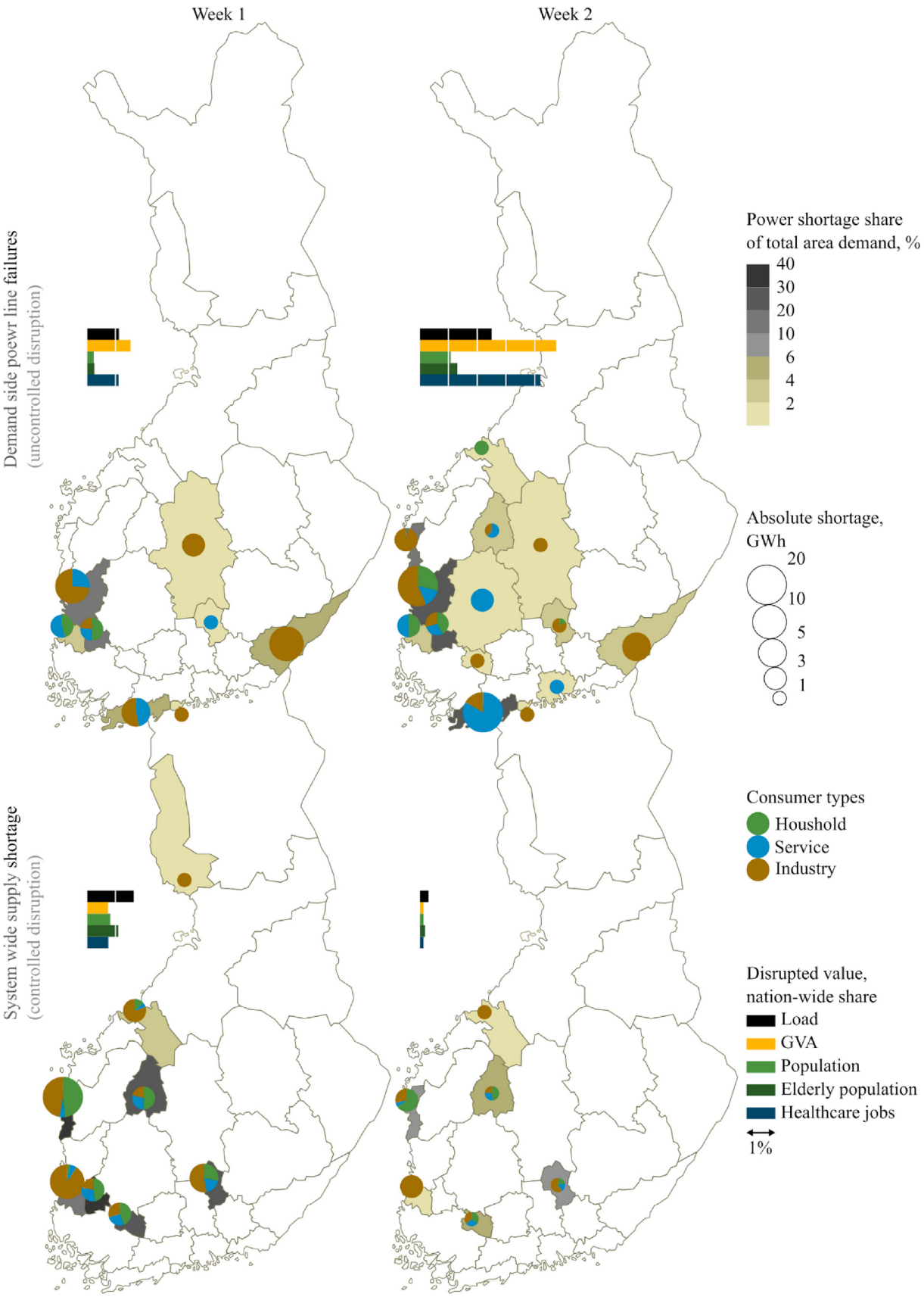

Fig. 14. Geographical and sectoral distribution of lost load and subsequently disrupted nation-wide shares of socio-economic values. Results are disaggregated by week and disruption type.

Table 3
Disrupted nation-wide shares of socio-economic values for different power disruption types and their ratio normalized by the disrupted power load.

	Socio-economic value	Week 1	Week 2
Failures	Load	1.10%	2.43%
	GVA	1.49%	4.72%
	Population	0.23%	1.06%
	Elderly population	0.28%	1.29%
	Healthcare jobs	1.09%	4.18%
Shortage	Load	1.61%	0.29%
	GVA	0.72%	0.12%
	Population	0.80%	0.12%
	Elderly population	1.08%	0.17%
	Healthcare jobs	0.71%	0.12%
$\frac{\left(\frac{Value}{Load}\right)_{failures}}{\left(\frac{Value}{Load}\right)_{shortage}}$	GVA	3.04	4.67
	Population	0.42	1.05
	Elderly population	0.38	0.91
	Healthcare jobs	2.24	4.01

population share in all cases is larger than the disrupted share of the whole population. The reason for this is the significantly older population structure in rural areas.

5. Conclusions

Here an integrated spatial modeling framework for linking disruptions in a power system with subsequent socio-economic impacts have been developed. The model was applied to an illustrative case in Finland.

The developed modeling framework provides new capabilities to study socio-economic costs of power disruptions using simple inter-layer links. The integrated link from the power system to the socio-economic parameters is a novel aspect of the framework as the power system models typically tend to focus only on techno-economic analyses. Both inter-layer links (from the natural environment describing threats to the energy system and from the energy system to the socio-economic values) are described through simple functions for each system component and consumer type that capture the most relevant relationships. Major challenges to accurately describe these link functions include (1) spatial aggregation of natural environment parameters with high local variability, (2) spatial aggregation of local grid fragility features, and (3) time dependency of socio-economic costs. A more rigorous derivation of the component fragilities and the social cost functions with uncertainties would improve the confidence in the representativeness of the model results.

The case study for Finland demonstrates the capabilities of the modeling framework for analyzing regional and sectorial distributions of power outages as well as their implications to people and businesses. The case concerns a two-week disturbance in the electricity system due to wind storm and limits on nuclear power and import capacities. The following observations and conclusions from the case study can be made:

- The cost of the power outage can be significantly reduced by controlling its location. Outage with controlled location resulted in 3–5 times lower economic loss than an uncontrolled outage. This is consistent with previous findings [23,24] and motivates prioritization of outage location when it is technically possible.
- Outage cost reduction potential is larger in control of consumer segments than in control of regions of the country even though the former may be more difficult to implement.
- Relative outage cost reduction potential decreases with an increasing level of disruption.
- The prioritization of one socio-economic value may increase the costs to another.

The economic loss to the businesses and social cost of disrupted healthcare services in the case study was partially reduced by increased social costs to households.

- The shift of outage between regions, while reducing the nation-wide costs, can systemically disadvantage certain regions during a system-wide shortage, potentially with higher share of vulnerable population.
- The choice of socio-economic value as a prioritization criterion is a critical decision, but its implications can be counterintuitive.

Consumer prioritization by population size of an area in the case study was affecting more people than a natural uncontrolled disruption did by disproportionally disconnecting commercial and industrial consumers.

The large variation in power outage costs, visible through higher granularity and dimensionality analysis, presents a potential to significantly reduce the costs of the outage by shifting the location of the outage and thus should be considered in addition to measures for minimizing the outage magnitude and duration. Measures to reduce the cost of the outage that do occur without reducing the outage itself are especially relevant for extreme and unexpected disruptions for which complete system protection is either not physically feasible or not economically justifiable. However, to gain an outage location optimization for the toolkit of outage cost mitigation measures would require certain aspects in the physical, organizational, and regulatory infrastructures. The most obvious prerequisite is a dense meshed grid topology with multiple lines reaching each consumer (or set of consumers). In Finland, most DGs have radial topology and thus the outage location optimization is possible only on a larger scale or for a few densely populated areas with meshed local grids. Adding connections within branches of local grids are expensive and are hard to justify even though this increases the reliability simply by providing another route from the main grid. However, there may be an economic case in some locations for meshed microgrids that have some local power production capacity to supply demand for at least critical functions in case they are disconnected from the main grid and are forced to operate in island mode. Enabling location optimization in either the national grid or local microgrids forced to operate with insufficient supply capacity requires a proper regulatory framework that allows and specifies rules for doing so. Also, system operators must be prepared for using such measures as they would have to be applied under time constraints of an emergency.

Further work will refine the modeling framework with improved representation of the natural environment, linking functions, and a more comprehensive list of socio-economic parameters. Also, more detailed resilience case studies are planned.

Credit author statement

Justinas Jasiunas: Formal analysis, Writing – original draft, Writing – review & editing, Visualization; Peter D. Lund: Conceptualization, Writing – review & editing, Supervision, Funding acquisition; Jani Mikkola: Software, Formal analysis, Writing – original draft; Liinu Koskela: Software.

Declaration of competing interest

The authors declare that they have no known competing financial interests or personal relationships that could have appeared to influence the work reported in this paper.

Acknowledgments

The financial support from the Research Council at the Academy of Finland (project WISE, grant number 312626) is greatly acknowledged.

Appendix A. Supplementary Information

Supplementary information to this article can be found online at https://doi.org/10.1016/j.energy.2021.119928.

References

[1] International Energy Agency. Digitalization & energy. https://doi.org/10.1787/9789264286276-en; 2017.
[2] International Energy Agency. World energy outlook 2018. 2018. https://doi.org/10.1787/weo-2018-en.
[3] Bompard E, Huang T, Wu Y, Cremenescu M. Classification and trend analysis of threats origins to the security of power systems. Int J Electr Power Energy Syst 2013;50:50–64. https://doi.org/10.1016/j.ijepes.2013.02.008.
[4] Ciscar JC, Dowling P. Integrated assessment of climate impacts and adaptation in the energy sector. Energy Econ 2014;46:531–8. https://doi.org/10.1016/j.eneco.2014.07.003.
[5] Gracceva F, Zeniewski P. A systemic approach to assessing energy security in a low-carbon EU energy system. Appl Energy 2014;123:335–48. https://doi.org/10.1016/j.apenergy.2013.12.018.
[6] Höltinger S, Mikovits C, Schmidt J, Baumgartner J, Arheimer B, Lindström G, et al. The impact of climatic extreme events on the feasibility of fully renewable power systems: a case study for Sweden. Energy 2019;178:695–713. https://doi.org/10.1016/j.energy.2019.04.128.
[7] Eder-Neuhauser P, Zseby T, Fabini J, Vormayr G. Cyber attack models for smart grid environments. Sustain Energy, Grids Netw 2017;12:10–29. https://doi.org/10.1016/j.segan.2017.08.002.
[8] Gorndon S, Goeckeler D, Hennessy J. Cybersecurity dialogue 2019. https://www.youtube.com/watch?v=J1t15Qs1NSA (accessed July 3, 2019).
[9] Sun CC, Hahn A, Liu CC. Cyber security of a power grid: state-of-the-art. Int J Electr Power Energy Syst 2018;99:45–56. https://doi.org/10.1016/j.ijepes.2017.12.020.
[10] Hosseini S, Barker K, Ramirez-Marquez JE. A review of definitions and measures of system resilience. Reliab Eng Syst Saf 2016;145:47–61. https://doi.org/10.1016/j.ress.2015.08.006.
[11] Jasiūnas J, Mikkola J, Lund PD. Energy system resilience – a review. Renew Sustain Energy Rev 2019. Submitted for publication.
[12] Fernández-Blanco Carramolino R, Careri F, Kavvadias K, Hidalgo-Gonzalez I, Zucker A, Peteves E. Systematic mapping of power system models. Exp Surv 2017. https://doi.org/10.2760/422399.
[13] Fu G, Wilkinson S, Dawson RJ, Fowler HJ, Kilsby C, Panteli M, et al. Integrated approach to assess the resilience of future electricity infrastructure networks to climate hazards. IEEE Syst J 2018;12:3169–80. https://doi.org/10.1109/JSYST.2017.2700791.
[14] Pfenninger S, Hawkes A, Keirstead J. Energy systems modeling for twenty-first century energy challenges. Renew Sustain Energy Rev 2014;33:74–86. https://doi.org/10.1016/j.rser.2014.02.003.
[15] Zachariadis T, Poullikkas A. The costs of power outages: a case study from Cyprus. Energy Pol 2012;51:630–41. https://doi.org/10.1016/j.enpol.2012.09.015.
[16] IEEE Standards Association. Std 1366TM-2012. New York: IEEE Guide for Electric Power Distribution Reliability Indices; 2012. https://doi.org/10.1109/IEEESTD.2012.6209381.
[17] Schröder T, Kuckshinrichs W. Value of lost load: an efficient economic indicator for power supply security? A literature review. Front Energy Res 2015;3:1–12. https://doi.org/10.3389/fenrg.2015.00055.
[18] Küfeoğlu S. Economic impacts of electric power outages and evaluation of customer interruption costs. Aalto University; 2015. https://doi.org/10.1109/ISGTEurope.2014.7028868.
[19] Ratha A, Iggland E, Andersson G. Value of Lost Load: how much is supply security worth? IEEE Power Energy Soc. Gen. Meet. 2013. https://doi.org/10.1109/PESMG.2013.6672826.
[20] Biskas PN, Bakirtzis GA, Chatziathanasiou V. Computation of strict long-run marginal cost for different HV consumers. Elec Power Syst Res 2015;128:66–78. https://doi.org/10.1016/j.epsr.2015.06.024.
[21] Hinojosa VH, Velásquez J. Stochastic security-constrained generation expansion planning based on linear distribution factors. Elec Power Syst Res 2016;140:139–46. https://doi.org/10.1016/j.epsr.2016.06.028.
[22] Aghaei J, Nikoobakht A, Siano P, Nayeripour M, Heidari A, Mardaneh M. Exploring the reliability effects on the short term AC security-constrained unit commitment: a stochastic evaluation. Energy 2016;114:1016–32. https://doi.org/10.1016/j.energy.2016.08.073.
[23] de Nooij M, Lieshout R, Koopmans C. Optimal blackouts: empirical results on reducing the social cost of electricity outages through efficient regional rationing. Energy Econ 2009;31:342–7. https://doi.org/10.1016/j.eneco.2008.11.004.
[24] Wolf A, Wenzel L. Welfare implications of power rationing: an application to Germany. Energy 2015;84:53–62. https://doi.org/10.1016/j.energy.2015.02.095.
[25] Becker S, Schober D, Wassermann S. How to approach consumers' nonmonetary evaluation of electricity supply security? The case of Germany from a multidisciplinary perspective. Util Pol 2016;42:74–84. https://doi.org/10.1016/j.jup.2016.06.012.
[26] Praktiknjo AJ, Hähnel A, Erdmann G. Assessing energy supply security: outage costs in private households. Energy Pol 2011;39:7825–33. https://doi.org/10.1016/j.enpol.2011.09.028.
[27] Panteli M, Mancarella P. Influence of extreme weather and climate change on the resilience of power systems: impacts and possible mitigation strategies. Elec Power Syst Res 2015;127:259–70. https://doi.org/10.1016/j.epsr.2015.06.012.
[28] Panteli M. Modeling and evaluating the resilience of critical electrical power infrastructure to extreme weather events. IEEE Syst J 2015;11:1733–42. https://doi.org/10.1109/JSYST.2015.2389272.
[29] Wang W, Lu Z. Cyber-security in smart grid: survey and challenges. Comput Electr Eng 2013;67:469–82. https://doi.org/10.1016/j.compeleceng.2018.01.015.
[30] Raman G, Peng JC-H, Rahwan T. Manipulating residents' behavior to attack the urban power distribution system. IEEE Trans Ind Inf 2019;15:1–12. https://doi.org/10.1109/tii.2019.2903882.
[31] Mitsova D, Esnard AM, Sapat A, Lai BS. Socioeconomic vulnerability and electric power restoration timelines in Florida: the case of Hurricane Irma. Nat Hazards 2018;94:689–709. https://doi.org/10.1007/s11069-018-3413-x.
[32] Haimila Kirsti, Nurmi Veli-Pekka, Virtanen Vesa. Electricity dependence in modern society (Sähköriippuvuus modernissa yhteiskunnassa). In: The Security Committee (Turvallisuuskomitea); 2015.
[33] Charani Shandiz S, Foliente G, Rismanchi B, Wachtel A, Jeffers RF. Resilience framework and metrics for energy master planning of communities. Energy 2020;203. https://doi.org/10.1016/j.energy.2020.117856.
[34] LaCommare KH, Eto JH, Dunn LN, Sohn MD. Improving the estimated cost of sustained power interruptions to electricity customers. Energy 2018;153:1038–47. https://doi.org/10.1016/j.energy.2018.04.082.
[35] Finnish Energy. Preparing for long disturbances n.d. https://energia.fi/energiasta/energiaverkot/sahkokatkot/pitkan_sahkokatkon_vaikutuksia (accessed June 20, 2020).
[36] Gholami A, Shekari T, Amirioun MH, Aminifar F, Amini MH, Sargolzaei A. Toward a consensus on the definition and taxonomy of power system resilience. IEEE Access 2018;6:32035–53. https://doi.org/10.1109/ACCESS.2018.2845378.
[37] Salman A. Risk-based assessment and strengthening of electric power systems subjected to natural hazards. Michigan Technological University; 2016.
[38] Francesco PEP, Cavalieri F, Franchin P, Vanzi I, Pitilakis K. Syner-G project. Deliverable D3.3 - fragility functions for electric power system elements. 2009.
[39] Panteli M, Mancarella P, Trakas DN, Kyriakides E, Hatziargyriou ND. Metrics and quantification of operational and infrastructure resilience in power systems. IEEE Trans Power Syst 2017;32:4732–42. https://doi.org/10.1109/TPWRS.2017.2664141.
[40] Niemi R, Lund PD. Decentralized electricity system sizing and placement in distribution networks. Appl Energy 2010;87:1865–9. https://doi.org/10.1016/j.apenergy.2009.11.002.
[41] Niemi RM, Lund PD. Alternative ways for voltage control in smart grids with distributed electricity generation. Int J Energy Res 2011;36:1032–43.
[42] Niemi R, Mikkola J, Lund PD. Urban energy systems with smart multi-carrier energy networks and renewable energy generation. Renew Energy 2012;48:524–36. https://doi.org/10.1016/j.renene.2012.05.017.
[43] Lee Willis H. Power distribution planning reference book, vol. 20044212; 2004. https://doi.org/10.1201/9781420030310.
[44] Espinoza S, Panteli M, Mancarella P, Rudnick H. Multi-phase assessment and adaptation of power systems resilience to natural hazards. Elec Power Syst Res 2016;136:352–61. https://doi.org/10.1016/j.epsr.2016.03.019.
[45] Paatero JV, Lund PD. Effects of large-scale photovoltaic power integration on electricity distribution networks. Renew Energy 2007;32:216–34. https://doi.org/10.1016/j.renene.2006.01.005.
[46] Energy Authority. Interruption statistics 2017. Keskeytystilasto 2017; 2018.
[47] Finnish Meteorological Institute. Download observations n.d. https://en.ilmatieteenlaitos.fi/download-observations#!/(accessed May 1, 2020).
[48] Fingrid. Open data on electricity market n.d. https://www.fingrid.fi/en/electricity-market/electricity-market-information/(accessed January 8, 2020).
[49] Finnish Energy. Structure of the electricity networks n.d. https://energia.fi/en/energy_sector_in_finland/energy_networks/electricity_networks (accessed July 8, 2020).
[50] Energy Authority. Security of Supply 2019. https://energiavirasto.fi/toimitusvarmuus (accessed January 9, 2020).
[51] Fingrid. Electricity system of Finland n.d. https://www.fingrid.fi/en/grid/power-transmission/electricity-system-of-finland/(accessed July 24, 2020).
[52] Finnish Energy. Finnish Energy n.d. https://energia.fi/(accessed January 9, 2020).
[53] Statistics Finland. Energy Year 2017 n.d. https://pxhopea2.stat.fi/sahkoiset_julkaisut/energia2018/html/engl0002.htm (accessed January 8, 2020).
[54] Fingrid. Power transmission grid of Fingrid. https://www.fingrid.fi/en/grid/

power-transmission/power-transmission-grid-of-fingrid/. [Accessed 16 December 2019].
[55] Dunn S, Wilkinson S, Alderson D, Fowler H, Galasso C. Fragility curves for assessing the resilience of electricity networks constructed from an extensive fault database. Nat Hazards Rev 2018;19. https://doi.org/10.1061/(ASCE)NH.1527-6996.0000267.
[56] Panteli M, Mancarella P. Operational resilience assessment of power systems under extreme weather and loading conditions. In: IEEE power energy soc. Gen. Meet, 2015– Septe. IEEE Computer Society; 2015. https://doi.org/10.1109/PESGM.2015.7286087.
[57] Panteli M, Trakas DN, Mancarella P, Hatziargyriou ND. Power systems resilience assessment: hardening and smart operational enhancement strategies. Proc IEEE 2017;105:1202–13. https://doi.org/10.1109/JPROC.2017.2691357.
[58] Panteli M, Trakas DN, Mancarella P, Hatziargyriou ND. Boosting the power grid resilience to extreme weather events using defensive islanding. IEEE Trans Smart Grid 2016;7:2913–22. https://doi.org/10.1109/TSG.2016.2535228.
[59] Forssén K. Resilience of Finnish electricity distribution networks against extreme weather conditions. Aalto University; 2016.
[60] Statistics Finland. Population n.d. http://tilastokeskus.fi/til/vrm_en.html (accessed January 9, 2020).
[61] Statistics Finland. Regional Account n.d. http://tilastokeskus.fi/til/altp/index_en.html (accessed January 9, 2020).
[62] Statistics Finland. PxWeb databases n.d. http://pxnet2.stat.fi/PXWeb/pxweb/en/StatFin/StatFin__vrm__tyokay/statfin_tyokay_pxt_115h.px/(accessed December 30, 2020).
[63] Fingrid. Impact of the winter storm on the grid 26-27 December 2011 2012. https://www.fingrid.fi/sivut/ajankohtaista/tiedotteet/2012/talvimyrskyn-vaikutukset-kantaverkkoon-26.-27.12.2011-paivitetty-9.1.2012/(accessed July 3, 2020).